International Journal of Greenhouse Gas Control 42 (2015) 554–561

Contents lists available at ScienceDirect

International Journal of Greenhouse Gas Control

journal homepage: www.elsevier.com/locate/ijggc

Tracing injected CO_2 in the Cranfield enhanced oil recovery field (MS, USA) using He, Ne and Ar isotopes

Domokos Györe[a,*], Finlay M. Stuart[a], Stuart M.V. Gilfillan[b], Susan Waldron[c]

[a] Isotope Geoscience Unit, Scottish Universities Environmental Research Centre, East Kilbride G75 0QF, UK
[b] School of GeoSciences, University of Edinburgh, Edinburgh EH9 3JW, UK
[c] School of Geographical and Earth Sciences, University of Glasgow, Glasgow G12 8QQ, UK

ARTICLE INFO

Article history:
Received 16 April 2015
Received in revised form 7 September 2015
Accepted 14 September 2015

Keywords:
Carbon capture and storage
Geological storage
Geochemical tracing
Carbon isotope
Noble gas isotope
Mass spectrometry

ABSTRACT

The He, Ne and Ar isotopic composition of gases collected in 2009 and 2012 from 13 production wells, injection wells and the CO_2 supply pipeline at the Cranfield CO_2-enhanced oil recovery field (MS, USA) have been measured in order to determine the extent to which they trace the fate of injected CO_2 in the reservoir. In the absence of samples of CO_2 pre-injection reservoir gas we use the Ne isotope composition of the production and injection well gases to determine the isotopic composition of the natural gas. The noble gas isotopes display binary mixing trends between the injected CO_2 and a CH_4-rich natural gas that is characterised by radiogenic He, Ne and Ar isotope ratios. $^3He/^4He$ and $^{40}Ar^*/^4He$ ratios (where $^{40}Ar^*$ represents the non-atmospheric ^{40}Ar) display coherent relationships with CO_2 concentrations that can be used to trace and quantify the injected CO_2 in an engineered site over a sustained period of injection. The presence of a small amount of air-derived Ar, from a non-atmospheric source, in many gas samples rules out using $^{40}Ar/^{36}Ar$ to track the injected CO_2. The noble gases identify the loss of a significant proportion of the CO_2 from the gas phase sampled by five production wells in 2009. Using $^3He/^4He$ and $^{40}Ar^*/^4He$ ratios to reconstruct the major gas composition, it appears that between 22% and 96% of the CO_2 has been lost in individual wells. This study demonstrates that the naturally occurring noble gases have the potential to trace the fate and quantify the sequestration of CO_2 at injection sites.

1. Introduction

Geological storage of CO_2 is the only means to directly reduce man-made CO_2 emissions to the atmosphere from industrial point sources (Scott et al., 2013). Developing techniques for monitoring and verifying the secure storage of injected CO_2 is essential if carbon capture and storage (CCS) is to become a realistic climate mitigation option. The verification process requires an understanding of the mechanism of storage and the ability to track the fate of CO_2 in the subsurface. Numerical simulations and laboratory experiments that model fluid flow, physical-chemical processes acting on the injected CO_2 (Ennis-King and Paterson, 2007; Knauss et al., 2005; White et al., 2005; Xu et al., 2005) and trapping mechanisms within engineered fields (Arts et al., 2004; Emberley et al., 2005) have been developed. These models require validation by field measurements.

Baseline studies at CCS test sites provide constraints on the movement of injected CO_2 (Stalker et al., 2015). Injection of CO_2 into depleted hydrocarbon fields has long been used for enhanced oil recovery (EOR). Given the large volumes of CO_2 transported and injected in these sites they can serve as analogues for geological CO_2 storage (Baines and Worden, 2004; Haszeldine et al., 2005). Additional insights on the storage and movement of anthropogenic gas can be acquired by studying naturally occurring CO_2 accumulations in the shallow crust (e.g. Gilfillan et al., 2008).

Several geochemical techniques have been developed for tracing the movement and storage of CO_2 in the crust (e.g. Humez et al., 2014 and references therein). The stable carbon isotope composition of CO_2 ($\delta^{13}C_{CO_2}$) has been widely and successfully used to trace injected gas, and track its interaction with reservoir fluid and rocks (Assayag et al., 2009; Johnson et al., 2011; Lu et al., 2012b; Myrttinen et al., 2010), as well as constrain the storage mechanism (e.g. Raistrick et al., 2006). However, the technique is less powerful if the $\delta^{13}C$ of the injected and in-place reservoir CO_2 are similar (e.g. Sherwood Lollar et al., 1997; Wycherley et al., 1999), or when CO_2 is liberated from carbonate reservoir rocks during reaction with the acidified formation water generated by CO_2 dissolution (Shevalier et al., 2013). Chemical tracers such as SF_6, perfluorocarbons and CD_4 have been added to CO_2 and used in CCS analogue studies to determine the timing of breakthrough of the injected gas (Stalker et al., 2015 and references therein).

* Corresponding author.
E-mail address: d.gyore.1@research.gla.ac.uk (D. Györe).

http://dx.doi.org/10.1016/j.ijggc.2015.09.009

The noble gases (He, Ne, Ar, Kr and Xe) are chemically inert and have several isotopes that allow them to be used to trace the physical processes that have affected crustal fluids, and to constrain gas residence time-scales. They have been used, for instance, to resolve the origin and movement of CO_2 in natural gas reservoirs (Gilfillan et al., 2009; Lafortune et al., 2009; Sathaye et al., 2014) as well as determine the long-term storage of CO_2 in natural gas fields (Ballentine et al., 2001; Gilfillan et al., 2008; Zhou et al., 2012). The addition of Kr and Xe isotopes to injected gas has been used to trace the movement of injected CO_2 in CCS trials (Lu et al., 2012a; Nimz and Hudson, 2005; Stalker et al., 2015).

The noble gases are present in trace amounts in natural CO_2 (e.g. Zhou et al., 2012). Where the isotopic composition of the noble gases in injected natural CO_2 are significantly different to those of the in-place reservoir gas they have the potential to trace the movement and mixing of the injected gas (Nimz and Hudson, 2005). Here we present the first comprehensive study to apply this technique in an EOR field that is an analogue for geologic CO_2 storage sites. We report the He, Ne and Ar isotope composition of well gases from the Cranfield EOR field, Mississippi, USA, over a period of three years after the start of CO_2 injection. The data allow us to trace the presence of injected CO_2 in the reservoir and the loss of a component of this injected CO_2.

2. The Cranfield oil and gas field

Cranfield is located in southwest Mississippi, ~20 km east of the town of Natchez (Fig. 1). The reservoir is an anticline of highly permeable fluvial sediments of the Upper Cretaceous Lower Tuscaloosa Formation. The reservoir rock is largely composed of 15–25 m thick

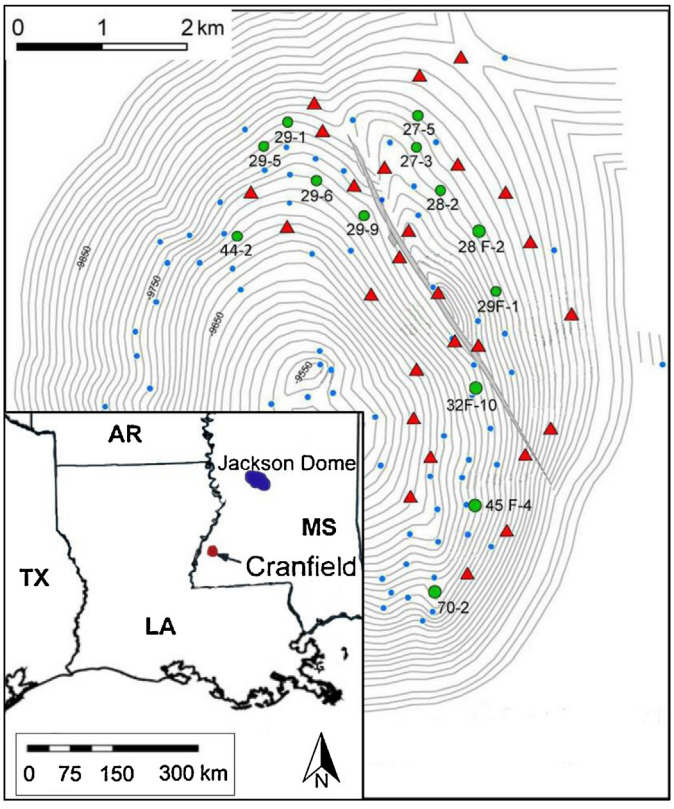

Fig. 1. Map of the Cranfield field, Mississippi, USA, showing the location of all injection wells (red triangles) and names of production wells sampled in this study (green circles). Unsampled wells are shown as small blue circles. Inset figure shows the location of the Cranfield site relative to the Jackson Dome field, the source of the injected CO_2. Redrawn after Lu et al. (2012b). (For interpretation of the references to colour in this figure legend, the reader is referred to the web version of this article.)

conglomerates, and occurs at depth of ~3000 m (Hosseini et al., 2013; Lu et al., 2012b). It was discovered in 1943 and oil and gas production commenced in 1944. The field is a simple dome structure (~6.4 km diameter), with a gas cap and associated down-dip oil ring. Pressure was maintained by gas recycling until the gas cap was depleted in 1959. It was abandoned in 1966 after unsuccessful water injection tests in 1958-59. The base and cap rock of the injection zone are low permeability mudstones. A SE–NW trending normal fault bisects the reservoir (Hovorka et al., 2013).

CO_2 injection for EOR started in July 2008 by Denbury Resources Incorporated. High purity (99%) CO_2 is transported ~160 km from the Jackson Dome deposit in central Mississippi (Fig. 1). CO_2 injection started at the north part of the field (Fig. 1) and extended to the southeast over the following three years. There was a corresponding development of injection and production wells to produce the oil mobilised by the CO_2 injection. Water and gas produced with the oil are separated at the surface on site. Produced water is disposed of via a deep water injection well, while the produced gas (CO_2 and CH_4) is mixed with Jackson Dome CO_2 and re-injected (this is termed recycled gas) (Choi et al., 2013).

In April 2010 the injection rate was approximately one million metric tonnes per year. By January 2013 6.8 million metric tonnes of CO_2 had been injected, of which 4 million had been retained in the reservoir (Hosseini et al., 2013; Hovorka et al., 2013). Between July 2009 and January 2013 the proportion of recycled gas in the injected gas had increased from ~9 to ~30% (Hovorka et al., 2013).

Prior to injection the reservoir re-equilibrated to hydrostatic pressure by groundwater infiltration over the ~40 years of abandonment. Continuous CO_2 injection without water injection means that Cranfield can be considered as an analogue for injection into a saline aquifer (Hovorka et al., 2011, 2013; Lu et al., 2012b). This is significant as saline formations offer the vast majority of available global CO_2 storage capacity (Scott et al., 2013). Consequently CO_2 monitoring and flow, sequestration modelling, trapping mechanism constraining and leak detection research have been undertaken extensively in the past few years (Hosseini et al., 2013; Hovorka et al., 2013; Lu et al., 2013; Nicot et al., 2013; Zhang et al., 2013, 2014). The binary mixing of the injected CO_2 with the naturally-occurring methane-rich reservoir gas is supported by $\delta^{13}C_{CO_2}$ measurements of produced gases (Lu et al., 2012b).

3. Sampling and analytical methods

The samples analysed for this study were collected in December 2009 and March 2012, 19 and 45 months after the start of CO_2 injection. Only the northeast part of the field was in operation during the first sampling trip. CO_2 injection and production was extended to the southeast by March 2012 (Fig. 1). The incoming pipeline from Jackson Dome to Cranfield (termed the bulkline) was sampled in 2012. Injection wells were sampled in both years with 22 gas samples being collected from production wells: 10 in 2009 and 12 in 2012. Nine of the 2009 wells were re-sampled in 2012 whilst three of the wells sampled in 2012 were not in use in 2009. Detailed well information is shown in Table 1.

The CO_2 in the bulkline and in the injection wells were maintained at around 21 MPa and 35 °C. Production wells were operated at between 0.8 and 9.1 MPa and around 60 °C. Oil, water and gas were present in the production wells therefore gas samples were taken from the top of the pipeline in order to avoid sampling liquid. Samples were collected in 8 mm outside diameter copper tubes that were connected to a pressure regulator using flexible pipe. The tube and gauge were flushed with gas for 5 min and then clamped at the end using a purpose built steel clamp, forming a cold weld. A similar clamp at the upstream end of the copper tube was closed

Table 1
Production and injection wells from the Cranfield EOR field sampled in this study.

Well ID	Well	Location	Latitude	Longitude	API number
31F-1	Injector	Franklin Co. SEC 31-T7N-R1E	31.563560	−91.141330	23-037-21488-0000
32F-4	Injector	Franklin Co. SEC 32-T7N-R1E	31.551200	−91.145650	23-037-21496-0100
27-3	Producer	Adams Co. SEC 27-T7N-R1W	31.579880	−91.160130	23-001-03394-0001
29F-1	Producer	Franklin Co. SEC 29-T7N-R1E	31.565364	−91.150319	23-037-00046-0001
29-5	Producer	Adams Co. SEC 29-T7N-R1W	31.580939	−91.179189	23-001-00173-0001
28-2	Producer	Adams Co. SEC 28-T7N-R1W	31.576350	−91.157210	23-001-23372-0000
28F-2	Producer	Franklin Co. SEC 28-T7N-R1W	31.572275	−91.153649	23-037-00048-0001
29-6	Producer	Adams Co. SEC 29-T7N-R1W	31.577300	−91.172600	23-001-00198-0001
29-9	Producer	Adams Co. SEC 29-T7N-R1W	31.573561	−91.166689	23-037-00159-0001
29-1	Producer	Adams Co. SEC 29-T7N-R1W	31.583589	−91.176239	23-001-00176-0001
27-5	Producer	Adams Co. SEC 27-T7N-R1W	31.583410	−91.159740	23-001-23380-0100
44-2	Producer	Adams Co. SEC 44-T7N-R1W	31.571200	−91.182660	23-001-23346-0000
45F-4	Producer	Franklin Co. SEC 45-T7N-R1E	31.541440	−91.153430	23-037-00336-0001
32F-10	Producer	Franklin Co. SEC 32-T7N-R1E	31.554860	−91.152940	23-037-00333-0000
70-2	Producer	Adams Co. SEC 70-T7N-R1W	31.537590	−91.155040	23-001-23410-1000

when the pressure reached 2–3 bar, again forming a cold weld and maintaining a helium tight seal.

Copper sample tubes were connected to an all-metal vacuum line maintained at ~35 °C and pumped to ultra high vacuum ($p < 10^{-7}$ mbar) using a turbo-molecular pump. The gas from the tube was expanded into a known volume and the absolute pressure was measured using a MKS 615-A Baratron capacitance manometer. The uncertainty on the pressure measurements is typically ±0.5% (1σ). A small fraction of the gas sample was used to determine the concentration of CO_2 and CH_4 using a Pfeiffer Vacuum QMS 200 quadrupole mass spectrometer. The mass spectrometer was calibrated by series of analyses of binary mixtures of CO_2 and CH_4 over the pressure range typical of samples. In several samples a small proportion of a sample gas was trapped into ~10 cm^3 glass tubes and CO_2 absorbed at −160 °C using liquid nitrogen and iso-pentane. Hydrocarbon gases were pumped off and $\delta^{13}C_{CO_2}$ was determined using a VG Optima dual inlet isotope ratios mass spectrometer in dynamic mode.

The remaining gas was expanded into a VG Scienta ST22 titanium sublimation pump that ran sequentially between ~900 °C and 15 °C. This purified gas was exposed to a SAES GP50 ZrAl alloy getter, held at 250 °C, for 20 min and subsequently expanded into a 0.5 litre reservoir. The concentration of ^{4}He, ^{20}Ne and ^{40}Ar were determined on the residual gas that was not trapped in the reservoir using the quadrupole mass spectrometer in order to guide subsequent isotopic analysis from the reservoir.

Typically He isotopes were measured in a ~1 cm^3 aliquot of gas from noble gas reservoir. This was purified by exposure to four hot GP50 ZrAl alloy getters and the heavy noble gases (Ar, Kr, Xe) were absorbed onto liquid nitrogen-cooled charcoal prior to analysis. Neon isotopes were typically measured in a larger volume of gas than for helium. Purification followed the procedure for He isotopes, except that Ne was trapped on charcoal at -243 °C for 20 min, helium was pumped off and the Ne released at −173 °C for 15 min prior to analysis. The gas was desorbed from the nitrogen-cooled charcoal by heating to room temperature for 15 min and the Ar isotope composition was determined.

The isotopic composition of the noble gases was measured by a MAP 215-50 mass spectrometer in static mode following established procedures (Codilean et al., 2008; Williams et al., 2005). ^{4}He, ^{36}Ar, ^{38}Ar and ^{40}Ar were measured on a Faraday detector with 10^{11} amplification, and ^{3}He, ^{20}Ne, ^{21}Ne, ^{22}Ne on a Burle channeltron electron multiplier in pulse counting mode at 2.5 kV. The hydrogen partial pressure was minimised by a room temperature GP50 getter in the mass spectrometer source volume. During He and Ne isotope analysis liquid nitrogen-cooled charcoal was used to minimise the heavy noble gases, hydrocarbons and CO_2 in the mass spectrometer.

The mass spectrometer sensitivity and mass fractionation was determined by repeated analysis of aliquots from reservoirs of HESJ international standard (Matsuda et al., 2002) for He, and air for Ne and Ar, during each analytical period. The reproducibility of noble gas isotope ratios and amounts presented in Table 2 are typically ±0.5% (1σ). Blanks for all isotopes were negligible.

4. Results

A sample of the bulkline gas taken in 2012 contains >99% CO_2 with a trace amount of CH_4 and noble gases. $\delta^{13}C_{CO_2}$ is −2.9‰, which is similar to previous determinations (Lu et al., 2012b; Zhou et al., 2012). The noble gas isotope ratios (Table 2) are similar to those measured from the Jackson Dome CO_2 deposit (Zhou et al., 2012).

The injected gases sampled in 2009 and 2012 are significantly different from the bulkline gas. The CO_2 content is lower; 96% in 2009 and 87% in 2012, with correspondingly higher CH_4 contents. ^{3}He/^{4}He (4.73–4.0R_A, where R_A is the atmospheric value of 1.39×10^{-6}) and ^{40}Ar/^{36}Ar (2906–2763) also decrease with time (Table 2). This is qualitatively consistent with the increased proportion of (methane-rich) reservoir gas in the injected gas as a result of recycling. ^{20}Ne/^{22}Ne and ^{21}Ne/^{22}Ne ratios do not change with time (10.61 and 10.69, and 0.035 and 0.037 respectively) taking experimental uncertainties at the 2σ level into account.

The gases from the production wells typically show an increase in the proportion of injected gas with time. This is apparent as an increase in the proportion of CO_2 in the nine wells that were sampled in both 2009 and 2012 (e.g. from 0.9 to 81.9% CO_2 in well 28F-2). This is mirrored by increases in ^{3}He/^{4}He, ^{20}Ne/^{22}Ne, ^{40}Ar/^{36}Ar and decreases in ^{21}Ne/^{22}Ne as well as ^{4}He, ^{20}Ne and ^{40}Ar concentrations (Table 2). In all the produced (and injected and bulkline) gas samples, ^{4}He/^{20}Ne ratios are at least five orders of magnitude higher than the atmospheric value ruling out any contamination from the atmosphere during field sampling or gas extraction from the Cu tube. $\delta^{13}C_{CO_2}$ measured in several gas samples (Table 2) is rather constant (−2.5 to −3‰). When plotted against CO_2 content (Fig. 2) the data are consistent with mixing of injected gas and the in-place reservoir gas with $\delta^{13}C_{CO_2} = -10.5$ ‰ determined previously (Lu et al., 2012b).

5. Discussion

5.1. Noble gas isotope systematics

Neon in natural gases is typically a mixture of three isotopically distinct sources: the crust, the mantle and the atmosphere (Ballentine and O'Nions, 1991). The Ne isotopic composition of CO_2

Table 2
Major gas, carbon isotope and noble gas isotope data from bulkline, injected and production well gases from the Cranfield EOR field.

Well	CO_2%	$\delta^{13}C_{CO_2}$ ‰ PDB	$^3He/^4He$ (R/R_A)	$^{20}Ne/^{22}Ne$	$^{21}Ne/^{22}Ne$	$^{40}Ar/^{36}Ar$	$^{38}Ar/^{36}Ar$	^4He ($\times10^{-4}$)	^{20}Ne ($\times10^{-9}$)	^{40}Ar ($\times10^{-5}$)
Bulkline	99.3	−2.96	5.32 (10)	10.82 (11)	0.0366 (2)	4331 (75)	0.188 (42)	0.100 (4)	0.57 (2)	0.60 (2)
Injector 2009	96.0	−2.49	4.73 (7)	10.61 (10)	0.0349 (7)	2906 (27)	0.185 (14)	0.79 (3)	9.07 (38)	4.27 (16)
Injector 2012	87.9	–	3.99 (6)	10.69 (10)	0.0372 (7)	2763 (10)	0.195 (7)	0.58 (2)	5.00 (21)	3.38 (13)
27-3 2009	81.0	−2.66	3.33 (5)	10.33 (13)	0.0382 (11)	1263 (9)	0.188 (6)	1.17 (4)	5.91 (25)	5.36 (20)
27-3 2012	82.3	–	3.39 (6)	10.54 (10)	0.0373 (8)	609 (2)	0.186 (4)	0.87 (3)	5.95 (25)	5.98 (22)
29F-1 2009	3.3	–	0.38 (1)	9.89 (10)	0.0388 (9)	910 (5)	0.190 (8)	2.83 (10)	13.32 (81)	6.54 (24)
29F-1 2012	70.5	–	2.18 (6)	10.30 (10)	0.0383 (7)	1565 (18)	0.187 (10)	1.17 (4)	7.76 (33)	4.26 (16)
29-5 2009	40.0	–	1.37 (3)	10.33 (10)	0.0377 (7)	1154 (5)	0.192 (5)	3.14 (9)	17.95 (76)	8.56 (32)
29-5 2012	85.5	–	3.92 (6)	10.66 (10)	0.0376 (7)	3126 (12)	0.190 (8)	0.77 (2)	5.71 (24)	3.46 (13)
28-2 2009	80.4	−2.48	2.75 (5)	10.46 (10)	0.0374 (7)	1989 (23)	0.189 (8)	0.91 (3)	6.50 (28)	3.75 (14)
28-2 2012	80.4	−3.10	2.77 (6)	10.49 (10)	0.0376 (8)	2017 (39)	0.190 (14)	0.94 (3)	6.47 (27)	3.77 (14)
28F-2 2009	0.9	–	0.21 (2)	9.79 (9)	0.0383 (8)	839 (6)	0.190 (10)	2.98 (11)	10.57 (45)	5.99 (22)
28F-2 2012	81.9	−2.43	3.22 (5)	10.43 (10)	0.0365 (7)	2123 (9)	0.196 (10)	0.87 (3)	7.20 (31)	3.57 (13)
29-6 2009	91.8	−2.52	4.18 (9)	10.93 (10)	0.0380 (8)	3671 (32)	0.186 (15)	0.89 (3)	7.15 (30)	4.32 (16)
29-6 2012	94.9	–	4.18 (9)	10.71 (10)	0.0370 (7)	3823 (31)	0.186 (24)	0.66 (2)	5.13 (22)	3.08 (11)
29-9 2009	94.9	−2.72	4.26 (9)	10.74 (10)	0.0365 (7)	3473 (17)	0.190 (18)	0.82 (3)	6.78 (29)	3.69 (14)
29-9 2012	82.4	–	3.46 (7)	10.62 (10)	0.0374 (8)	2306 (36)	0.190 (29)	0.90 (3)	5.70 (24)	3.88 (14)
29-1 2009	80.7	–	2.85 (6)	10.45 (10)	0.0373 (8)	2012 (17)	0.190 (13)	1.04 (4)	7.63 (32)	3.99 (15)
29-1 2012	82.0	−2.55	3.23 (8)	10.62 (10)	0.0375 (8)	2604 (9)	0.190 (15)	0.95 (3)	6.71 (28)	4.15 (15)
27-5 2009	46.9	–	1.71 (4)	10.08 (9)	0.0373 (8)	1348 (11)	0.190 (6)	0.92 (3)	5.26 (22)	4.17 (15)
27-5 2012	82.5	–	2.85 (5)	10.56 (10)	0.0376 (8)	2592 (17)	0.180 (16)	1.01 (4)	6.29 (27)	3.64 (13)
44-2 2009	8.4	–	0.69 (2)	9.92 (9)	0.0376 (7)	1133 (5)	0.190 (8)	3.12 (11)	14.37 (61)	9.66 (36)
45F-4 2012	81.6	−2.58	2.90 (7)	10.51 (10)	0.0375 (8)	2427 (29)	0.200 (20)	0.83 (3)	5.99 (25)	3.77 (14)
32F-10 2012	80.3	–	2.91 (6)	10.62 (10)	0.0362 (7)	2156 (14)	0.202 (9)	0.96 (4)	6.46 (27)	3.15 (12)
70-2 2012	83.4	–	3.18 (8)	10.51 (9)	0.0371 (7)	2486 (34)	0.184 (16)	0.95 (3)	6.44 (27)	3.61 (13)
AIR			1.000 (9)	9.81(8)	0.0290 (3)	298.6 (3)	0.1885 (3)	0.052 (1)	16452 (36)	930 (1)

Uncertainties (1σ) in last significant figures are in parentheses. Relative uncertainties of CO_2 measurements are 1%, while the absolute uncertainty of $\delta^{13}C_{CO_2}$ is ±0.17‰. The composition of air is after Eberhardt et al. (1965), Mamyrin et al. (1970) and Mark et al. (2011). Standard conditions are after Ozima and Podosek (2001). Noble gas concentrations are fraction of volume and are given in cm^3 (STP)/cm^3.

from the Jackson Dome field is a mixture of mantle-derived Ne with air-derived Ne that has been isotopically fractionated prior to mixing (Zhou et al., 2012). Previous measurements of Jackson Dome gas are plotted on Fig. 3, with a grey dashed line showing the mixing trend. The Ne isotope composition of gases from the injection and production wells from Cranfield define a trend between a point on the Jackson Dome mixing line that is indistinguishable from the measured bulkline gas ($^{20}Ne/^{22}Ne = 10.92$; $^{21}Ne/^{22}Ne = 0.037$), and a point along a mixing line between air and crustal (radiogenic) Ne that must represent the in-place natural gas (Fig. 3). Following Ballentine et al. (2005), a best-fit line through the data, using the least square method can be used to determine the Ne isotope composition of the natural gas end-member ($^{20}Ne/^{22}Ne = 9.62 \pm 0.02$ and $^{21}Ne/^{22}Ne = 0.0384 \pm 0.001$).

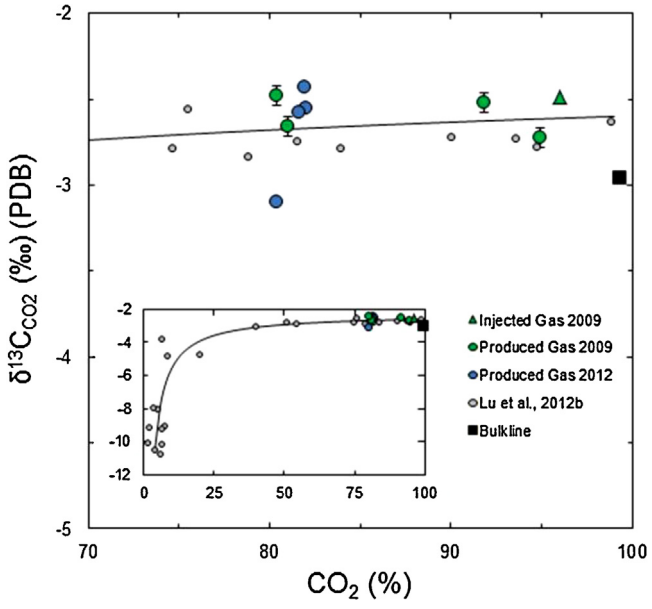

Fig. 2. Plot of $\delta^{13}C_{CO_2}$ (‰) vs. CO_2 concentration for production well gases from the Cranfield field. The mixing curve in inset figure is that generated by Lu et al. (2012b) for mixing of a natural gas with 4% CO_2 and $\delta^{13}C = -10.5$‰ and bulkline composition of 99.3% CO_2 and $\delta^{13}C = -2.6$‰. 1σ uncertainties are smaller than symbols.

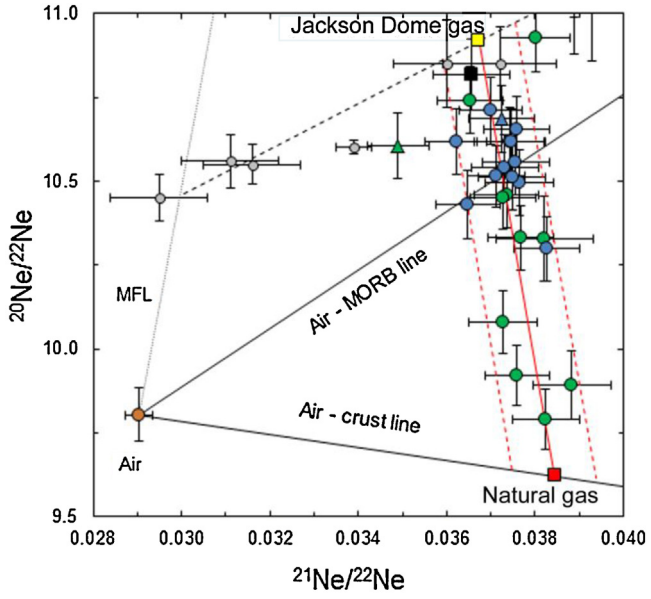

Fig. 3. The Ne three-isotope plot of gases from the Cranfield EOR site. The data plot as a binary mixture between injected gas, which is similar to the composition of Jackson Dome CO_2 (Zhou et al., 2012), and reservoir gas which plots on the air-crust mixing line. The best-fit mixing line (red line) defines the composition of the reservoir gas ($^{20}Ne/^{22}Ne = 9.62 \pm 0.02$; $^{21}Ne/^{22}Ne = 0.0384 \pm 0.001$). The red dashed lines represent the 1σ uncertainty of the best-fit line. Black square: bulkline, triangle: injected gas, circle: produced gas, green: 2009, blue: 2012. Grey circles represent Jackson Dome CO_2 data from Zhou et al. (2012) and the red (natural gas) and yellow (Jackson Dome) squares represent the end-member Ne isotope compositions. MFL: mass fractionation line. All uncertainties are 1σ. (For interpretation of the references to colour in this figure legend, the reader is referred to the web version of this article.)

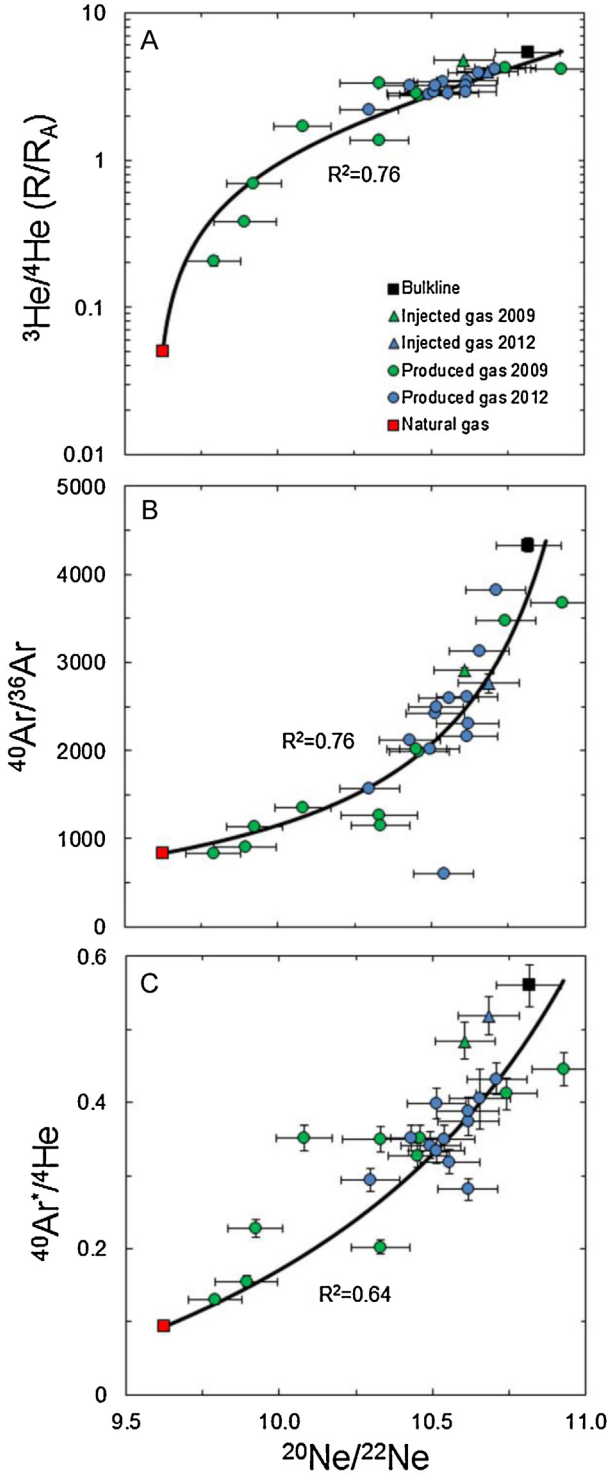

Fig. 4. $^{20}Ne/^{22}Ne$ of produced and injection well gases from the Cranfield EOR site plotted against (A) $^{3}He/^{4}He$, (B) $^{40}Ar/^{36}Ar$ and (C) $^{40}Ar^{*}/^{4}He$. The He and Ar isotope composition of the natural gas end-member (red square) is determined is determined based on the previously determined $^{20}Ne/^{22}Ne$ of natural gas end-member (9.62) and the best fit line defined by the data. Uncertainties are 1σ. (For interpretation of the references to colour in this figure legend, the reader is referred to the web version of this article.)

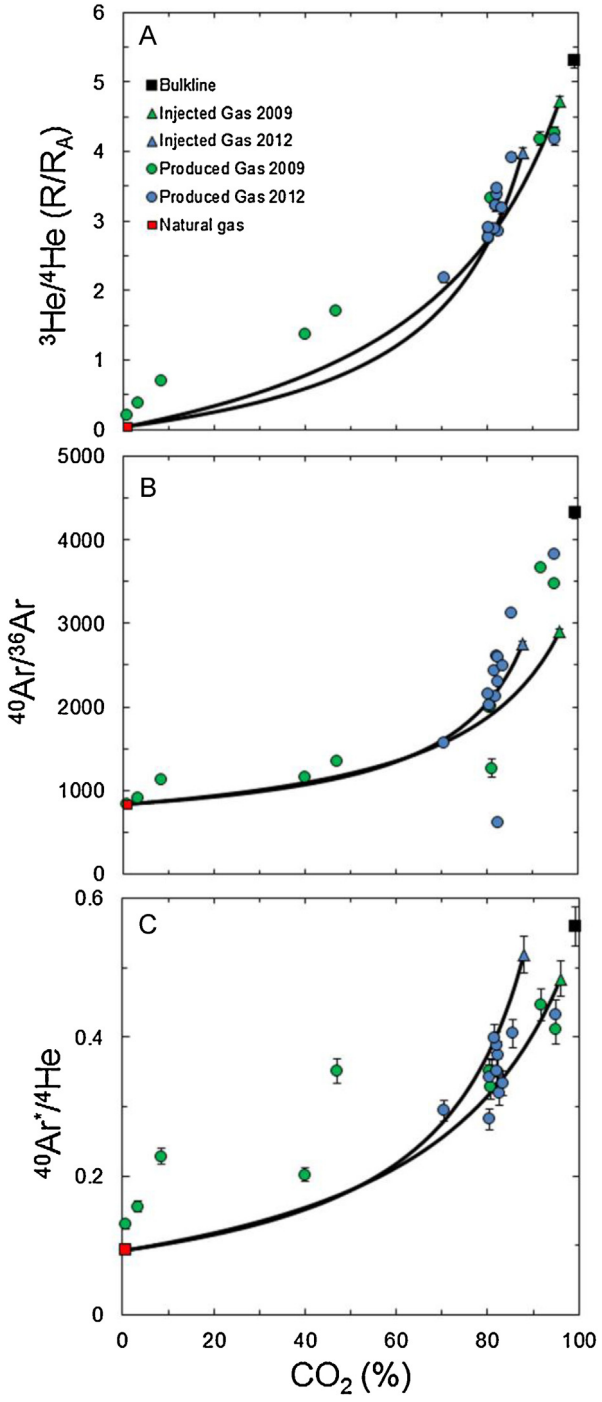

Fig. 5. The CO_2 content of the produced and injection well gases plotted against (A) $^{3}He/^{4}He$, (B) $^{40}Ar/^{36}Ar$ and (C) $^{40}Ar^{*}/^{4}He$. The natural gas end-member (red square) is determined using the best-fit line (black solid line) defined by the measured (injection wells) and calculated (reservoir gas) isotopic compositions and concentrations (see main text for details). Uncertainties are 1σ. (For interpretation of the references to colour in this figure legend, the reader is referred to the web version of this article.)

The identification of this end-member allows us to determine the He and Ar isotopic composition of the in-place natural gas by plotting values against $^{20}Ne/^{22}Ne$ (Fig. 4). These values are insensitive to natural variation in the crustal $^{21}Ne/^{22}Ne$. For instance, if we use the highest crustal $^{21}Ne/^{22}Ne$ (0.76) instead of 0.52 (Ballentine, 1997) the $^{20}Ne/^{22}Ne$ of the reservoir gas is 9.68 ± 0.02. This minor shift has no significant impact on the He and Ar isotope composition of the reservoir gas (Fig. 4) and the interpretation of noble gas-CO_2 data (Fig. 5).

Fig. 4A shows the $^{3}He/^{4}He$ ratio of the injected and production well gases plotted against $^{20}Ne/^{22}Ne$ ratios. The data, in particular the production well gases from 2012, define a trend that is

consistent with a binary mixture of injected gas and the in-place reservoir gas. Using the Ne isotope composition of the end-members defined above, the best-fit mixing curve defines the $^{3}He/^{4}He$ of the natural gas of $0.05 \pm 0.005R_A$. This value is close to the average ratio of continental crust ($\sim 0.02R_A$; after Andrews, 1985) and is lower than the lowest measured $^{3}He/^{4}He$ in the production well gases (28F-2 2009; $0.2R_A$). The hyperbolic nature of the mixing curve indicates that the $^{3}He/^{4}He$ of the natural gas end-member is rather poorly defined. The degree of the curvature of the mixing line is defined by $^{4}He/^{22}Ne_{Jackson\ Dome}/^{4}He/^{22}Ne_{natural\ gas}$ (0.488). Combining this value with the measured $^{4}He/^{22}Ne$ of the Jackson Dome gas (12,452; Zhou et al., 2012), the $^{4}He/^{22}Ne$ of the natural gas is 25,524. The lowest CO_2 sample has measured $^{4}He/^{22}Ne = 28{,}178$ which is consistent with the calculated value.

Using a similar technique, the $^{40}Ar/^{36}Ar$ of the natural gas end-member can be obtained (Fig. 4B). Although the Ne–Ar isotope data is not as coherent as the He–Ne isotope data, the data is also consistent with mixing between the injected gas and reservoir gas. The best-fit line defines the natural gas $^{40}Ar/^{36}Ar$ of 836 ± 75. This is higher than the atmospheric $^{40}Ar/^{36}Ar$ (298.6; Mark et al., 2011) and is consistent with the presence of a significant concentration of crust-derived radiogenic ^{40}Ar in the natural gas. The curvature of the mixing line is defined by $^{36}Ar/^{22}Ne_{Jackson\ Dome}/^{36}Ar/^{22}Ne_{natural\ gas} = 0.2$. Combining this value with the measured $^{36}Ar/^{22}Ne$ of the Jackson Dome gas (8.36), the $^{36}Ar/^{22}Ne$ of the natural gas is 41.7.

Air-derived noble gases are present to varying extents as a third component that tends to obscure the mixing trend in Ne–Ar isotope space (e.g. well 27-3, Fig. 4B). The $^{20}Ne/^{36}Ar$ data close to air-saturated water values are suggesting that the atmospheric noble gases likely originate from degassed formation water rather than directly from air. The low concentration of He in air (5.24×10^{-6} cm^3 (STP)/cm^3) means that air addition has no significant effect in Fig. 4A. The atmospheric ^{40}Ar contribution can be removed leaving radiogenic Ar, denoted as $^{40}Ar^*$ (Stuart and Turner, 1992). A plot of $^{40}Ar^*/^{4}He$ vs. $^{20}Ne/^{22}Ne$ reveals a coherent trend (Fig. 4C) that yields a $^{40}Ar^*/^{4}He = 0.09 \pm 0.01$ for the natural gas end-member.

The He, Ne and Ar isotope compositions of the in-place gas end-member are radiogenic, and strongly indicative of a crustal source with no resolvable mantle-derived volatiles. This is typical of natural gas accumulations from stable continental cratons (Prinzhofer, 2013). The $^{40}Ar^*/^{4}He$ is significantly lower than produced in normal continental crust ($\sim$0.2; e.g. Torgersen et al., 1989) and likely reflects the preferential release of ^{4}He from minerals in the reservoir rocks at lower temperature than ^{40}Ar by diffusion and/or ejection of α-particles.

5.2. Tracking the fate of injected CO_2

The coherent relationships between noble gas isotope compositions in the produced gas (Figs. 3 and 4) support the hypothetical binary mixture between the injected gas and in-place gas. Consequently the naturally occurring noble gases have the potential to trace the injected CO_2. A plot of the noble gas isotope ratios against the molar proportion of CO_2 in the gas samples helps to elucidate the relationship (Fig. 5).

The helium isotopic composition of the production well gases is plotted against the CO_2 content (Fig. 5A). Theoretical mixing curves are drawn between the 2009 and 2012 injected gases and a natural gas end-member ($^{3}He/^{4}He = 0.05R_A$). The curvature of the mixing lines are calculated using the measured ^{4}He concentration in the injected gas (Table 2) and the natural gas, which is assumed to be that of the lowest CO_2 sample (28F-2 2009; 3×10^{-4} cm^3 (STP)/cm^3). The 2009 and 2012 mixing lines overlap as the evolution of the injected gas mirrors the mixing of in situ and injected gases in the reservoir. With the exception of the five lowest CO_2 concentration 2009 samples, the data plot within the field defined by the mixing curves and are consistent with the predicted two-component mixing. This demonstrates that He isotopes fingerprint the injected CO_2 and have the potential to be used as a tracer of fugitive emissions of CO_2 from CCS sites where there is significant difference between the helium isotopic composition of the injected and in-place gases.

The $^{40}Ar/^{36}Ar$ of the production well gases are plotted against CO_2 content in Fig. 5B along with theoretical mixing lines between the 2009 and 2012 injected gas composition with the in-place natural gas. As in Fig. 5A, the mixing curves are defined by data from the injectors and the $^{40}Ar/^{36}Ar$ of the natural gas (836) determined from the Ar–Ne isotope relationship (Fig. 4B). The concentration of ^{36}Ar of the reservoir gas is taken from the lowest CO_2 sample (28F-2 2009; 7×10^{-8} cm^3 (STP)/cm^3). Few data plot on the mixing line, and the systematic relationship observed for $^{3}He/^{4}He$–CO_2 is not apparent. For instance, the four low CO_2 samples plot above the mixing line, as observed in Fig. 5A. Gas samples from well 27-3 taken in 2009 and 2012 plot significantly below the mixing curve. This may be due to the addition of small amount of air-derived Ar that will tend to lower $^{40}Ar/^{36}Ar$ ratios but have little effect on CO_2 due to its low concentration in air. In addition, four samples (two from each sampling campaign) have higher $^{40}Ar/^{36}Ar$ than the injected gases, yet below the value of Jackson Dome CO_2 from the bulkline. This implies that the production wells are tapping gas that was injected earlier than that sampled at the injectors, when the Ar isotope composition of the injected gas was closer to that of Jackson Dome CO_2 as the presence of atmospheric air contamination has been ruled out by the consistently high $^{4}He/^{20}Ne$ ratios.

The $^{40}Ar^*/^{4}He$ ratio allows the effect of small contributions of air-derived Ar to be removed (e.g. Stuart and Turner, 1992). The $^{40}Ar^*/^{4}He$ is plotted vs. CO_2 along with theoretical mixing lines between the injected gas and a natural gas end-members in Fig. 5C. The curvature of each mixing line is defined by the concentration of ^{4}He (see above). The data generally follow the mixing lines to a greater extent than Ar isotopes. As observed previously, the five low CO_2 samples plot above the hypothetical mixing line.

The low CO_2 concentration gases sampled in 2009 are the general exception to the systematic mixing relationships identified in CO_2 vs. $^{3}He/^{4}He$ and $^{40}Ar^*/^{4}He$ (Fig. 5). In all cases, including the CO_2 vs. $^{40}Ar/^{36}Ar$ plot, the data plot significantly above the mixing lines. The internal consistency of the noble gas isotope data (Fig. 4) implies that this is unlikely to be the result of the addition of another noble gas component. The simplest and most likely explanation is that it reflects the loss of CO_2 from the gas phase during the early phase of CO_2 injection. The proportion of CO_2 that has been lost can be quantified using the measured $^{3}He/^{4}He$ and $^{40}Ar^*/^{4}He$ ratios. The distance on the ordinate between the data point and the mixing curve in Fig. 5 represents the absolute change in CO_2 concentration. The proportion lost (%) is calculated by normalising to the predicted CO_2 content. For instance, gas from well 28F-2 2009 has 0.8% CO_2 and $^{3}He/^{4}He$ of $0.21R_A$. The 2009 mixing curve for that $^{3}He/^{4}He$ predicts 11.8% CO_2, equating to a loss of 93%. The predicted CO_2 concentrations and the lost proportion have been calculated using $^{3}He/^{4}He$ and $^{40}Ar^*/^{4}He$ ratios (Table 3 and Fig. 6).

The $^{3}He/^{4}He$ data require the loss of between 28% (27-5 2009) and 93% (28F-2 2009) of the injected CO_2 from the gas phase. From the $^{40}Ar^*/^{4}He$ this range is 22–96%. The degree of CO_2 loss from each sample calculated from the two tracers appears to be broadly consistent (Fig. 6). Uncertainties have been propagated by taking into account the uncertainty of CO_2 concentration and noble gas isotope ratios of each sample, and the mixing curve uncertainty which originates from the uncertainty of the end-member compositions. It should be noted that any process that causes CO_2 loss

Table 3
The measured and reconstructed CO_2 concentrations from the five lowest CO_2 samples. Estimated uncertainties are 2σ.

Well	Measured CO_2%	Calculated CO_2% from $^3He/^4He$	CO_2 loss (%) from $^3He/^4He$	Calculated CO_2% from $^{40}Ar^*/^4He$	CO_2 loss (%) from $^{40}Ar^*/^4He$
28F-2 2009	0.9	12 (4)	93 (4)	23 (6)	96 (4)
29F-1 2009	3.3	22 (4)	85 (4)	35 (6)	91 (4)
44-2 2009	8.4	37 (5)	77 (4)	58 (5)	86 (6)
29-5 2009	40.0	58 (4)	30 (8)	51 (5)	22 (8)
27-5 2009	46.9	65 (4)	28 (6)	81 (5)	42 (4)

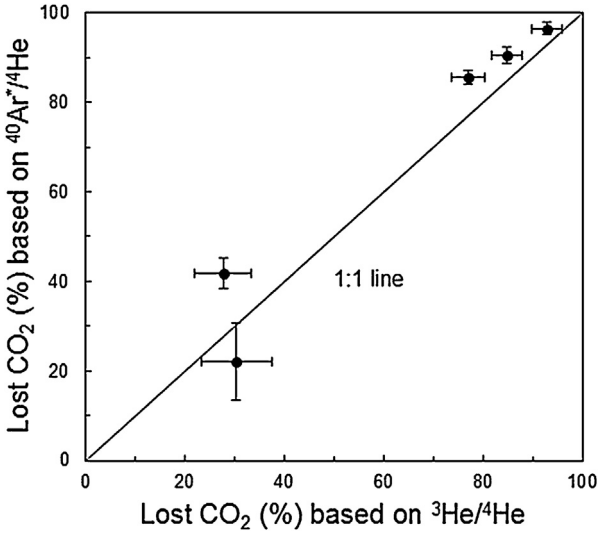

Fig. 6. Plot showing the loss of CO_2 from some 2009 well gases calculated from the difference between measured $^3He/^4He$ and $^{40}Ar^*/^4He$ ratios and those predicted from the mixing lines. Uncertainties are 2σ.

may fractionate the $^{40}Ar^*/^4He$ ratio of the residual gas. We do not take that into account here as it is likely negligible compared to the changes in CO_2 concentration.

Whilst the mechanism by which CO_2 has been sequestered (e.g. dissolution into the formation water, precipitation as carbonate, residual trapping) is not the aim of this study, the data provide a clear indication that the naturally-occurring noble gases have the potential to track the fate of injected CO_2 in future CCS trials. Further work will examine this topic in detail but is outside the scope of the current work.

6. Conclusions

The unique noble gas isotope composition of the Jackson Dome CO_2 injected in the Cranfield CO_2-EOR field permits evaluation of the effectiveness of using He, Ne and Ar isotopes to trace injected CO_2. The isotopic compositions of production well gases sampled in 2009 and 2012, 19 and 45 months after the start of CO_2 injection define binary mixtures between injected gas and the in-place reservoir gas. This allows the noble gas isotopic composition of the reservoir gas to be determined. $^3He/^4He$ and $^{40}Ar^*/^4He$ of produced gas samples plot on theoretical mixing lines with CO_2 content indicating that the noble gas isotopes track the presence of the injected CO_2. The five sample with the lowest proportion of CO_2 sampled in 2009 plot consistently above the theoretical mixing lines. This requires the loss of 22–96% of the injected CO_2 from the gas phase, and suggests that the noble gas isotopes have potential to quantify the storage of CO_2 in CCS sites. The total amount of sequestered CO_2 and the sequestration mechanism is currently unresolved but is the focus of ongoing work.

Acknowledgements

We thank Denbury Resources Inc. for permission to sample and providing assistance in the field and Susan Hovorka for assistance in obtaining this permission. We thank Jiemin Lu for providing useful detailed background information on the field. The work was funded by EPSRC, grant number EP/K036033/1. Thanks to Terry Donnelly and Luigia Di Nicola for invaluable help in the laboratories. We thank Chris Ballentine and an anonymous reviewer for helpful and constructive reviews which have greatly improved the manuscript.

References

Andrews, J.N., 1985. The isotopic composition of radiogenic helium and its use to study groundwater movement in confined aquifers. Chem. Geol. 49, 339–351.
Arts, R., Eiken, O., Chadwick, A., Zweigel, P., van der Meer, L., Zinszner, B., 2004. Monitoring of CO_2 injected at Sleipner using time-lapse seismic data. Energy 29, 1383–1392.
Assayag, N., Matter, J., Ader, M., Goldberg, D., Agrinier, P., 2009. Water–rock interactions during a CO_2 injection field-test: implications on host rock dissolution and alteration effects. Chem. Geol. 265, 227–235.
Baines, S.J., Worden, R.H., 2004. The Long-term Fate of CO_2 in the Subsurface: Natural Analogues for CO_2 Storage, vol. 233. Geological Society, London, pp. 59–85 (special publications).
Ballentine, C.J., 1997. Resolving the mantle He/Ne and crustal $^{21}Ne/^{22}Ne$ in well gases. Earth Planet. Sci. Lett. 152, 233–249.
Ballentine, C.J., Marty, B., Sherwood Lollar, B., Cassidy, M., 2005. Neon isotopes constrain convection and volatile origin in the Earth's mantle. Nature 433, 33–38.
Ballentine, C.J., O'Nions, R.K., 1991. The nature of mantle neon contributions to Vienna Basin hydrocarbon reservoirs. Earth Planet. Sci. Lett. 113, 553–567.
Ballentine, C.J., Schoell, M., Coleman, D., Cain, B.A., 2001. 300-Myr-old magmatic CO_2 in natural gas reservoirs of the west Texas Permian basin. Nature 409, 327–331.
Choi, J.-W., Nicot, J.-P., Hosseini, S.A., Clift, S.J., Hovorka, S.D., 2013. CO_2 recycling accounting and EOR operation scheduling to assist in storage capacity assessment at a U.S. gulf coast depleted reservoir. Int. J. Greenh. Gas Control 18, 474–484.
Codilean, A.T., Bishop, P., Stuart, F.M., Hoey, T.B., Fabel, D., Freeman, S.P.H.T., 2008. Single-grain cosmogenic ^{21}Ne concentrations in fluvial sediments reveal spatially variable erosion rates. Geology 36, 159.
Eberhardt, P., Eugster, O., Marti, K., 1965. A redetermination of the isotopic composition of atmospheric neon. Z. Naturforsh. 20a, 623–624.
Emberley, S., Hutcheon, I., Shevalier, M., Durocher, K., Mayer, B., Gunter, W.D., Perkins, E.H., 2005. Monitoring of fluid–rock interaction and CO_2 storage through produced fluid sampling at the Weyburn CO_2-injection enhanced oil recovery site, Saskatchewan, Canada. Appl. Geochem. 20, 1131–1157.
Ennis-King, J., Paterson, L., 2007. Coupling of geochemical reactions and convective mixing in the long-term geological storage of carbon dioxide. Int. J. Greenh. Gas Control 1, 86–93.
Gilfillan, S.M.V., Ballentine, C.J., Holland, G., Blagburn, D., Sherwood Lollar, B., Scott, S., Schoell, M., Cassidy, M., 2008. The noble gas geochemistry of natural CO_2 gas reservoirs from the Colorado Plateau and Rocky Mountain provinces, USA. Geochim. Cosmochim. Acta 72, 1174–1198.
Gilfillan, S.M.V., Sherwood Lollar, B., Holland, G., Blagburn, D., Stevens, S., Schoell, M., Cassidy, M., Ding, Z., Zhou, Z., Lacrampe-Couloume, G., Ballentine, C.J., 2009. Solubility trapping in formation water as dominant CO_2 sink in natural gas fields. Nature 458, 614–618.
Haszeldine, R.S., Quinn, Q., England, G., Wilkinson, M., Shipton, Z.K., Evans, J.P., Heath, J., Crossey, L., Ballentine, C.J., Graham, C.M., 2005. Natural geochemical analogues for carbon dioxide storage in deep geological porous reservoirs, a United Kingdom perspective. Oil Gas Sci. Technol. – Rev. IFP 60, 33–49.
Hosseini, S.A., Lashgari, H., Choi, J.W., Nicot, J.-P., Lu, J., Hovorka, S.D., 2013. Static and dynamic reservoir modeling for geological CO_2 sequestration at Cranfield, Mississippi, U.S.A. Int. J. Greenh. Gas Control 18, 449–462.

Hovorka, S.D., Meckel, T.A., Treviño, R.H., 2013. Monitoring a large-volume injection at Cranfield, Mississippi—Project design and recommendations. Int. J. Greenh. Gas Control 18, 345–360.
Hovorka, S.D., Meckel, T.A., Trevino, R.H., Lu, J., Nicot, J.-P., Choi, J.-W., Freeman, D., Cook, P., Daley, T.M., Ajo-Franklin, J.B., Freifeild, B.M., Doughty, C., Carrigan, C.R., Brecque, D.L., Kharaka, Y.K., Thordsen, J.J., Phelps, T.J., Yang, C., Romanak, K.D., Zhang, T., Holt, R.M., Lindler, J.S., Butsch, R.J., 2011. Monitoring a large volume CO_2 injection: year two results from SECARB project at Denbury's Cranfield, Mississippi, USA. Energy Procedia 4, 3478–3485.
Humez, P., Lions, J., Négrel, P., Lagneau, V., 2014. CO_2 intrusion in freshwater aquifers: review of geochemical tracers and monitoring tools, classical uses and innovative approaches. Appl. Geochem.
Johnson, G., Mayer, B., Shevalier, M., Nightingale, M., Hutcheon, I., 2011. Tracing the movement of CO_2 injected into a mature oilfield using carbon isotope abundance ratios: the example of the Pembina Cardium CO_2 Monitoring project. Int. J. Greenh. Gas Control 5, 933–941.
Knauss, K.G., Johnson, J.W., Steefel, C.I., 2005. Evaluation of the impact of CO_2, co-contaminant gas, aqueous fluid and reservoir rock interactions on the geologic sequestration of CO_2. Chem. Geol. 217, 339–350.
Lafortune, S., Moreira, M., Agrinier, P., Bonneville, A., Schneider, H., Catalette, H., 2009. Noble gases as tools for subsurface monitoring of CO_2 leakage. Energy Procedia 1, 2185–2192.
Lu, J., Cook, P.J., Hosseini, S.A., Yang, C., Romanak, K.D., Zhang, T., Freifeld, B.M., Smyth, R.C., Zeng, H., Hovorka, S.D., 2012a. Complex fluid flow revealed by monitoring CO_2 injection in a fluvial formation. J. Geophys. Res. Solid Earth 117.
Lu, J., Kharaka, Y.K., Thordsen, J.J., Horita, J., Karamalidis, A., Griffith, C., Hakala, J.A., Ambats, G., Cole, D.R., Phelps, T.J., Manning, M.A., Cook, P.J., Hovorka, S.D., 2012b. CO_2–rock–brine interactions in lower Tuscaloosa formation at Cranfield CO_2 sequestration site, Mississippi, U.S.A. Chem. Geol. 291, 269–277.
Lu, J., Kordi, M., Hovorka, S.D., Meckel, T.A., Christopher, C.A., 2013. Reservoir characterization and complications for trapping mechanisms at Cranfield CO_2 injection site. Int. J. Greenh. Gas Control 18, 361–374.
Mamyrin, B.A., Anufrijev, G.S., Kamenskii, I.L., Tolstikhin, I.N., 1970. Determination of the isotopic composition of atmospheric helium. Geochem. Int. 7, 498–505.
Mark, D.F., Stuart, F.M., de Podesta, M., 2011. New high-precision measurements of the isotopic composition of atmospheric argon. Geochim. Cosmochim. Acta 75, 7494–7501.
Matsuda, J., Matsumoto, T., Sumino, H., Nagao, K., Yamamoto, J., Miura, Y., Kaneoka, I., Takahata, N., Sano, Y., 2002. The $^3He/^4He$ ratio of the new internal He Standard of Japan (HESJ). Geochem. J. 36, 191–195.
Myrttinen, A., Becker, V., van Geldern, R., Würdemann, H., Morozova, D., Zimmer, M., Taubald, H., Blum, P., Barth, J.A.C., 2010. Carbon and oxygen isotope indications for CO_2 behaviour after injection: first results from the Ketzin site (Germany). Int. J. Greenh. Gas Control 4, 1000–1006.
Nicot, J.-P., Oldenburg, C.M., Houseworth, J.E., Choi, J.-W., 2013. Analysis of potential leakage pathways at the Cranfield, MS, U.S.A., CO_2 sequestration site. Int. J. Greenh. Gas Control 18, 388–400.
Nimz, G.J., Hudson, G.B., 2005. The use of noble gas isotopes for monitoring leakage of geologically stored CO_2. In: Thomas, D.C., Benson, S.M. (Eds.), Carbon Dioxide Capture for Storage in Deep Geologic Formations. Elsevier, pp. 1113–1128.
Ozima, M., Podosek, F.A., 2001. Noble Gas Geochemistry, 2nd ed. Cambridge University Press, Cambridge, pp. 367.
Prinzhofer, A., 2013. Noble gas in oil and gas accumuations. In: Burnard, P. (Ed.), The Noble Gases as Geochemical Tracers. , pp. 225–247.
Raistrick, M., Mayer, B., Shevalier, M., Perez, R.J., Hutcheon, I., Perkins, E., Gunter, B., 2006. Using chemical and isotopic data to quantify ionic trapping of injected carbon dioxide in oil field brines. Environ. Sci. Technol. 40, 6744–6749.
Sathaye, K.J., Hesse, M.A., Cassidy, M., Stockli, D.F., 2014. Constraints on the magnitude and rate of CO_2 dissolution at Bravo Dome natural gas field. PNAS 111 (43), 15332–15337.
Scott, V., Gilfillan, S., Markusson, N., Chalmers, H., Haszeldine, R.S., 2013. Last chance for carbon capture and storage. Nat. Clim. Change 3, 105–111.
Sherwood Lollar, B., Ballentine, C.J., O'Nions, R.K., 1997. The fate of mantle-derived carbon in a continental sedimentary basin: integration of C/He relationships and stable isotope signatures. Geochim. Cosmochim. Acta 61, 2295–2307.
Shevalier, M., Nightingale, M., Mayer, B., Hutcheon, I., Durocher, K., Perkins, E., 2013. Brine geochemistry changes induced by CO_2 injection observed over a 10 year period in the Weyburn oil field. Int. J. Greenh. Gas Control 16, S160–S176.
Stalker, L., Boreham, C., Underschultz, J., Freifeld, B., Perkins, E., Schacht, U., Sharma, S., 2015. Application of tracers to measure, monitor and verify breakthrough of sequestered CO_2 at the CO2CRC Otway Project, Victoria, Australia. Chem. Geol. 399, 2–19.
Stuart, F.M., Turner, G., 1992. The abundance and isotopic composition of the noble gases in ancient fluids. Chem. Geol. 101, 97–109.
Torgersen, T., Kennedy, B.M., Hiyagon, H., Chiou, K.Y., Reynolds, J.H., Clarke, W.B., 1989. Argon accumulation and the crustal degassin flux of ^{40}Ar in the Great Artesian Basin, Australia. Earth Planet. Sci. Lett. 92, 43–56.
White, S.P., Allis, R.G., Moore, J., Chidsey, T., Morgan, C., Gwynn, W., Adams, M., 2005. Simulation of reactive transport of injected CO_2 on the Colorado Plateau, Utah, USA. Chem. Geol. 217, 387–405.
Williams, A.J., Stuart, F.M., Day, S.J., Phillips, W.M., 2005. Using pyroxene microphenocrysts to determine cosmogenic ^3He concentrations in old volcanic rocks: an example of landscape development in central Gran Canaria. Quat. Sci. Rev. 24, 211–222.
Wycherley, H., Fleet, A., Shaw, H., 1999. Some observations on the origins of large volumes of carbon dioxide accumulations in sedimentary basins. Mar. Petrol. Geol. 16, 489–494.
Xu, T., Apps, J.A., Pruess, K., 2005. Mineral sequestration of carbon dioxide in a sandstone–shale system. Chem. Geol. 217, 295–318.
Zhang, R., Ghosh, R., Sen, M.K., Srinivasan, S., 2013. Time-lapse surface seismic inversion with thin bed resolution for monitoring CO_2 sequestration: a case study from Cranfield, Mississippi. Int. J. Greenh. Gas Control 18, 430–438.
Zhang, R., Sen, M.K., Srinivasan, S., 2014. Time-lapse pre-stack seismic inversion with thin bed resolution for CO_2 sequestration from Cranfield, Mississippi. Int. J. Greenh. Gas Control 20, 223–229.
Zhou, Z., Ballentine, C.J., Schoell, M., Stevens, S.H., 2012. Identifying and quantifying natural CO_2 sequestration processes over geological timescales: the Jackson Dome CO_2 Deposit, USA. Geochim. Cosmochim. Acta 86, 257–275.